Basic Research in Cardiology (2019) 114:30
https://doi.org/10.1007/s00395-019-0739-9

ORIGINAL CONTRIBUTION

Relaxin mitigates microvascular damage and inflammation following cardiac ischemia–reperfusion

Xiao-Ming Gao[1,2,3,4] · Yidan Su[1] · Shirley Moore[1] · Li-Ping Han[1] · Helen Kiriazis[1] · Qun Lu[1] · Wei-Bo Zhao[1] · Amanguli Ruze[2,3] · Bin-Bin Fang[2,3] · Ming-Jun Duan[2,3] · Xiao-Jun Du[1]

Received: 17 November 2018 / Accepted: 14 June 2019 / Published online: 19 June 2019

Abstract

Microvascular obstruction (MVO) and leakage (MVL) forms a pivotal part of microvascular damage following cardiac ischemia–reperfusion (IR). We tested the effect of relaxin therapy on MVO and MVL in mice following cardiac IR injury including severity of MVO and MVL, opening capillaries, infarct size, regional inflammation, cardiac function and remodelling, and permeability of cultured endothelial monolayer. Compared to vehicle group, relaxin treatment (50 µg/kg) reduced no-reflow area by 38% and the content of Evans blue as a permeability tracer by 56% in jeopardized myocardium (both $P < 0.05$), effects associated with increased opening capillaries. Relaxin also decreased leukocyte density, gene expression of cytokines, and mitigated IR-induced decrease in protein content of VE-cadherin and relaxin receptor. Infarct size was comparable between the two groups. At 2 weeks post-IR, relaxin treatment partially preserved cardiac contractile function and limited chamber dilatation versus untreated controls by echocardiography. Endothelial cell permeability assay demonstrated that relaxin attenuated leakage induced by hypoxia-reoxygenation, H_2O_2, or cytokines, action that was independent of nitric oxide but associated with the preservation of VE-cadherin. In conclusion, relaxin therapy attenuates IR-induced MVO and MVL and endothelial leakage. This protection was associated with reduced regional inflammatory responses and consequently led to alleviated adverse cardiac remodeling.

Keywords Microvascular obstruction · Microvascular leakage · Microvascular damage · Ischemia–reperfusion · Relaxin · Cardiac remodeling

Introduction

Microvascular damage represents a pivotal part of myocardial ischemia–reperfusion (IR) injury that may limit overall therapeutic efficacy for myocardial preservation. Manifestation of microvascular damage consists of two aspects likely with distinct consequences, microvascular obstruction (MVO) also known as "no-reflow" and microvascular leakage (MVL) [13, 16, 31]. Clinical studies using angiogram (TIMI score) or cardiac magnetic resonance (CMR) imaging have shown that MVO occurs in approximately 30–60% patients with acute myocardial infarction (MI) received reperfusion therapy including primary percutaneous coronary intervention (PCI) [20, 26]. Patients with signs of no-reflow post-PCI exhibit a four–sixfold increase in the risk for major adverse cardiovascular events [36]. Current understanding on the mechanism of microvascular damage is limited but several factors are regarded as important including endothelial cell swelling, platelet activation, formation

Electronic supplementary material The online version of this article (https://doi.org/10.1007/s00395-019-0739-9) contains supplementary material, which is available to authorized users.

✉ Xiao-Ming Gao
xiaoming.gao@baker.edu.au

✉ Xiao-Jun Du
xiao-jun.du@baker.edu.au

1 Experimental Cardiology Laboratory, Baker Heart and Diabetes Institute, 75 Commercial Road, Melbourne, VIC 3004, Australia

2 State Key Laboratory of Pathogenesis, Prevention and Treatment of High Incidence Diseases in Central Asia, Ürümqi, China

3 Xinjiang Key Laboratory of Medical Animal Model Research, Clinical Medical Research Institute of Xinjiang Medical University, Ürümqi, China

4 Department of Surgery, Central Clinical School, Monash University, Melbourne, Australia

of microthrombi, inflammatory cell adhesion and external compression of capillaries due to regional oedema [5, 31].

While MVO has received intense investigation, MVL, has been much less studied. A strict and selective microvascular permeability is critical to tissue health [29]. Recent clinical CMR studies have documented the presence of intra-myocardial oedema and haemorrhage, which is regarded as a consequence of loss of microvascular integrity [8]. Increased vascular permeability could promote regional inflammatory infiltration and oedema with the latter further reduces blood perfusion of the jeopardised myocardium [13, 20, 36]. Factors such as intracellular signalling evoked by inflammatory and endothelial cell–cell interaction, oxidative stress, alteration of endothelial junction molecules, detachment of pericytes from microvasculature could all contribute to microvascular hyper-permeability [31, 45]. Unfortunately, there has been no effective therapy for microvascular damage.

Relaxin, a peptide hormone, is important in reproductive physiology [30]. During the last decades, broader protective actions of relaxin to different organs have been documented in a variety of pathological settings including oxidative stress, inflammation, diabetes, anaphylaxis and post-injury organ fibrosis [14, 15]. Cardiac protection by relaxin treatment against myocardial damage following I/R has also been reported [3, 46], albeit microvascular damage was not studied. Relaxin's actions on vascular endothelial cells involve upregulation of nitric oxide (NO) production [1, 10], anti-inflammation [4] and anti-platelet activity [2]. Thus, the pleiotropic actions of relaxin are expected to work synergistically in limiting microvascular damage following cardiac IR injury. In this study, we tested in mouse IR model, the therapeutic effect of relaxin on cardiac microvascular damage and explored potential mechanisms.

Materials and methods

Animals, surgery and relaxin treatment

Male C57Bl/6 mice at 12–14 weeks of age were used. All experimental procedures were approved by Alfred and Monash Research Education Precinct (AMREP) Animal Ethics Committee complied with the National Health and Medical Research Council of Australia Code for the Care and Use of Animals for Scientific Purposes (8th edition). Following our previous report and the recently published guideline papers [6, 23, 33], open-chest surgery was performed to occlude the left coronary artery for a designated period (e.g. 1 h or 4 h) followed by release of the occlusion for reperfusion for varying periods [6, 23, 33]. Detailed experimental protocols are shown in Fig. 1.

To determine in vivo dosage of relaxin, human recombinant relaxin peptide (provided by Novartis AG), we conducted a pilot experiment testing effect of different dosages of relaxin on MVL. Mice were subjected to 1 h ischemia followed by reperfusion to 24 h. Relaxin was administered as a bolus i.p. (15, 50, 150 µg/kg) immediately after coronary artery occlusion. Considering a short half-life of relaxin (approximately 2 h), relaxin was administered intraperitoneally after coronary artery occlusion as a bolus followed by continuously delivery of relaxin at 15, 50, 150 µg/kg/day, respectively, through osmotic minipump (Alzet, USA) subcutaneously implanted before reperfusion [42]. The 50 µg/kg of relaxin treatment was shown to reach the maximal reduction of Evans blue leakage in the LV (Supplementary Fig. 1), therefore, this dose was chosen for the in vivo study.

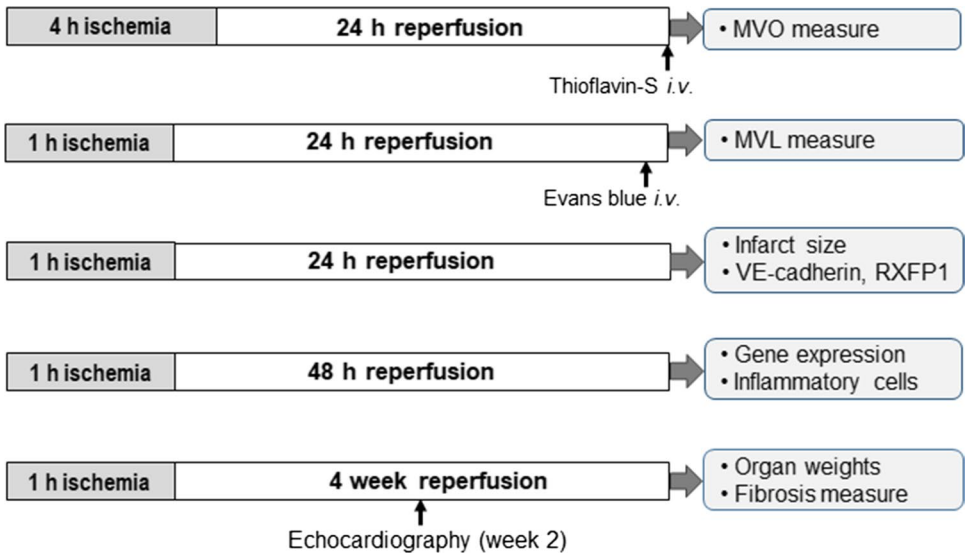

Fig. 1 Schematic diagram showing protocols applied for different experiments. Sham-operated mice matched with experimental duration served as controls

Measurement of microvascular obstruction

Effect of relaxin therapy on MVO was determined using the dual-staining method as previously described [23, 41]. In brief, at the end of IR (4 h/24 h), mice were anesthetized and ventilated. The chest was re-opened and a ligation suture was re-positioned at the same occlusion site of the left coronary artery. Then a fluorescent dye, thioflavin-S (4%, 0.1 ml in bolus), was injected via the inferior vena cava immediately followed by re-occlusion of the coronary artery. Evans blue (3%, 0.15 ml) was then injected via an aortic cannula to stain the non-ischemic myocardium. The heart was harvested and washed to remove excessive Evans blue dye. The LV was isolated, frozen on dry ice and cut into 7–8 slices (0.8 mm in thickness). LV sections were mounted on glass slides and exposed to UV light (302 nm) using a UV transilluminator for digital imaging. Area at risk (AAR, absence of Evans blue staining) and areas with MVO (attenuated or absence of thioflavin-S fluorescence) were determined using ImageJ software. MVO area was expressed as percentage of AAR.

Histological measurement of microvascular leakage

Evans blue (20 mg/kg, Sigma) as a tracer of microvascular permeability was given via a tail vein before termination. Evans blue in the left ventricle (LV) was extracted and measured as described in the following section [22, 23]. The size and the severity of MVL were determined using the methods as we previously described [23]. Following IR (1 h/24 h), and at 3 h before termination of the experiment, Evans blue dye (20 mg/kg, about 0.1 ml per animal) was injected intravenously allowing the blue dye permeated into the interstitial space of the ischemic myocardium through the leaking microvessels. At the end, the chest was opened and the aorta cannulated. Saline (approximately 2 ml) was slowly flushed through the coronary vasculature to remove blood containing Evans blue until effluent become colourless. The heart was then excised, frozen on dry ice, transversely sliced into 7–8 sections at 0.8–1 mm in the thickness, and compressed between two glass slides for digital photography. The entire blue-stained area (total MVL) or dark and light blue-stained areas (severe or mild MVL) at each section were measured using Image-Pro Analyzer 7.0.1 (Media Cybernetics, Inc. USA) and ImageJ software and were expressed as the percentage of the LV, respectively.

Chromatographic quantification microvascular leakage

Tissue content of Evans blue was determined as we previously described [22, 23]. In brief, after photography of LV serial sections, blue-stained myocardium was separated from non-stained tissues under a dissecting microscope and weighed. The blue stained myocardium was minced, digested in 50% trichloroacetic acid (Sigma) and homogenized with an assistance of metal beads to fully dissolve the blue dye. The supernatant was removed to a fresh tube after centrifugation and 100 µl of each sample was added to a 96-well plate in duplicates. Content of Evans blue was determined using a Bio-Rad microplate spectrophotometer. Absorbance at 620 nm filter was measured and calculated against the Evans blue standard. Evans blue in the sample was normalized by tissue wet weight (µg/mg).

Measurement of lumen-opening capillaries in the border zone

The number of lumen-opening capillaries was determined by immunohistochemistry using fresh frozen LV sections after IR (1 h/24 h). Briefly, LV sections were incubated with protein block solution (DAKO protein block serum-free) and then incubated with Alexa Fluor® 568 isolectin GS-IB_4 conjugate (1:10 dilution, Invitrogen, Aust.) at 4 °C overnight to stain endothelial cells. After PBS wash, sections were incubated with WGA-FITC solution (1:50 dilution) to stain myocyte membrane for 2 h and then mounted with anti-fade mounting media. Using an Olympus BX61 fluorescence microscope, 8–10 independent images (20 × magnification) from each LV section were acquired from the border zone of the infarct area. Under microscope, non-infarct zone (NIZ) and the infarct zone (IZ) can be clearly differentiated by signs such as muscle fiber disarray and presence of gaps between muscle fibres. We select areas between the IZ and the NIZ as the border zone for capillary analysis. This is because microstructures are better preserved within the border zone compared to the central IZ. Determination of lumen-open or lumen-close capillaries was judged by the visibility of the lumen of a capillary in blinded fashion. The number of lumen-open or -closed capillaries were manually counted, normalized to the cross-section tissue area of each image and expressed as the percentage of lumen-opening capillaries in total number of capillaries per high-magnification-filed.

Determination of regional inflammation

Immunohistochemistry for density of leukocytes

This assay was performed using hearts of mice with IR (1 h/48 h). Regional density of infiltrated leukocytes was measured in fresh frozen LVs by immunofluorescent staining for CD45 cells (leukocytes). Briefly, LV sections (5 µm in thickness) were incubated with rat anti-mouse CD45 (1:50, BD Biosciences) as primary antibody, followed by secondary antibody Alexa Fluor® 546 goat anti-rat IgG (1:500 red florescence, Life Technologies). ProLong® Gold antifade

reagent with nuclear acid dye DAPI (blue fluorescence, Invitrogen) was added to each sample to stain for nuclei. Co-localisation of the two fluorescence colours turned to purple colour identifying $CD45^+$ cells. Images were acquired using an Olympus BX61 fluorescence microscope and leukocyte density was analysed, in a blinded fashion, using Image-Pro Analyzer software and expressed as average cell number per mm^2, as we described previously [22, 50].

Enzyme-linked immunosorbent assay

Blood was collected through the cardiac puncture with heparin as the anticoagulant at the termination. Plasma levels of IL-1β, IL-6 and TNF-α were measured by Enzyme-linked immunosorbent assay (ELISA), in duplicates, using commercial mouse Duoset ELISA kits (all products of R&D System), according to the manufacture's instructions [21, 22, 50].

Gene expression by real-time PCR

RNA was extracted from LV tissue using Trizol® Reagent (Sigma). RNA (1 µg) was used for cDNA synthesis and quantitative PCR was performed using SYBR Green Master Mix qPCR (Roche, Germany) and target primers (Sigma). Gene expression level was normalized to that of GAPDH or TATA-Box Binding Protein Associated Factor 8 using the method of $2^{-\Delta\Delta ct}$, and presented relative to that of control value. Expression of the following genes were determined: interleukin-1β (IL-1β), IL-6, tumor necrosis factor-α (TNF-α), monocyte chemotactic protein 1 (MCP-1), vascular endothelial growth factor (VEGF) and relaxin family peptide receptor 1 (RXFP1) by quantitative real-time PCR (qPCR) using Applied Biosystems 7500 fast real-time PCR system. Results were normalised to house-keeping genes (18s or GAPDH), as previously described [22, 50].

Quantitative histological analysis of infarct size and fibrosis

Infarct size measurement

Infarct size was determined by a dual-staining method as we described previously [21]. Following IR (1 h/24 h), animals were anesthetized and the chest was opened. After aortic cannulation, saline was flushed through coronary vessels to wash away the blood. The left coronary artery was re-occluded at the original ligation position and 3% Evans blue (0.1 ml) was retrogradely injected through the ascending aorta to stain the non-ischemic myocardium, which differs from MVL determination using Evans blue dye as a tracer of microvascular permeability. After Evans blue injection, the LV was harvested immediately, frozen on dry ice and transversely cut into 6–7 sections. LV sections were incubated with 1.5% triphenyltetrazolium chloride (TTC) for 45 min to identify ischemic but viable myocardium (red) and dead myocardium (pale). LV sections were compressed between two glass slides and digital photos were acquired. The blue stained area (non-ischemic myocardium) and areas stained red and pale were measured using ImageJ software. The following formulas were used for the calculation of (1) area at risk (AAR) = (red area + pale area)/(blue area + red area + pale area); and (2) infarct size = pale area/(red area + pale area).

Assessment of cardiac fibrosis

The LV from mice with IR (1 h/4 weeks) was collected, paraffin embedded and serially cut into 7–8 sections (5 µm) from the apex to the base per sample at the interval of 0.8 mm. Picrosirius Red staining was performed to identify myocardial fibrosis. Digital images (10× magnification) were acquired and red stained areas (indicating collagen deposition) in each LV sections were measured using Image-Pro Analyzer software and expressed as percentage of total LV area [50].

Echocardiography

At the end of IR (1 h/2 week), mice were anesthetized using 1.7% isoflurane. Transthoracic echocardiography was performed using the Vevo 2100 ultrasound system (Visualsonics, Toronto, Canada) equipped with a 40 MHz linear-array transducer. A long axis view of the LV was obtained, as we previously described [23]. To assess cardiac remodeling and dysfunction, LV cross-sectional area at end-systole or end-diastole (LVESA, LVEDA) and LV volumes at end-systole or end-diastole (LVESV, LVEDV) were measured from 2D long-axis images and fractional area change (FAC%) and ejection fractional (EF%) was calculated by the Vevo echo software. Images were analysed by a single investigator in a blinded fashion and double checked by another experienced researcher.

Cell culture model for endothelial cell permeability assay

Endothelial cells from the mouse heart immortalized endothelial cells line (H5V) [24] were cultured in DMEM with serum and glucose in the upper-chamber for 7 days to confluence. Permeability across endothelial cell monolayer was measured in transwell units (with polycarbonate filter, 0.4 µm pore; Corning Costar) under following conditions in the presence or absence of relaxin (100 ng/ml): (1) 6 h hypoxia, (2) 6 h hypoxia followed by re-oxygenation for 1 h, 6 h or 24 h, respectively, (3) H_2O_2 (500 µM) for 15 h,

(4) IL-1β (10 ng/ml) for 15 h or (5) microphage migration inhibitory factor (MIF, 5 ng/ml) for 15 h. FITC-dextran (0.5 mg/ml, average molecular mass 40,000; Sigma) as a fluorescent indicator was added into the upper-chamber for 2 h before the end of the 15 h period. The amount of FITC-dextran appeared in the lower chamber was determined for the assessment of endothelial cell leakage. At the indicated time points, 100 µl sample was taken from the lower-chamber and the fluorescence of FITC-dextran was measured (485/535 nm, absorption/emission wavelengths) on EnSpire™ Multimode Reader to reflect the permeability of endothelial cell layer.

For hypoxia experiments, the transwell unit with endothelial monolayer was incubated in serum-free and glucose-free DMEM and placed in a hypoxic chamber (Modular Incubator chamber MIC-101, QNA International Pty Ltd, Australia) saturated with a 5% CO_2, 95% N_2 gaseous mix. The chamber was kept in an incubator with humid condition and warmed at 37 °C [40]. At the end of 6 h hypoxia, the cells were reoxygenated for various durations by incubation in normoxic conditions in glucose-containing, serum-free DMEM. Control normoxic cultures were also prepared.

In another set of cell experiment, nitric oxide (NO)-dependency of relaxin's endothelial protection was tested. Using the same transwell system, cultured endothelial cells were subjected to hypoxia for 6 h or stimulated with MIF for 15 h together with addition of NO scavenger, hydroxocobalamin (HXC, 100 µM). Then 100 µl sample was taken from the lower-chamber and the fluorescence of FITC-dextran was measured.

Immunoblotting

Expression levels of VE-cadherin and RXFP1 were measured by immunoblotting in H5V endothelial cells (6 h hypoxia) and also in the ischemic myocardium (IR 1 h/24 h). Proteins enriched with membrane fractions were extracted as previously described [35]. Heart tissue and cells were lysed in an SDS buffer (0.125 M Tris–Cl, 15% glycerine, 4% SDS), homogenised and sonicated. Lysates were then centrifuged at 12,000*g* for 8 min to remove cellular debris. The supernatant was extracted to determine total protein concentration by BCA method (Thermo Scientific). 50–100 µg of proteins were separated by 4–15% mini-PROTEAN TGX-Stain free gels (Bio-Rad) and blotted onto a PVDF membrane (Millipore). Membranes were blocked with blocking buffer (5% dried milk, 0.05% gelatine, 1% bovine serum albumin, 0.1% Tween-20, 1 × Tris-buffered saline solution) at room temperature for 2 h and then incubated at 4 °C overnight with primary anti-bodies against VE-cadherin (1:1000, Affymetrix eBioscience) or RXFP1 (1:1000, IMGENEX). Secondary antibodies such as goat anti-rabbit IgG-HRP (1:3000, Bio-Rad); goat anti-rat IgG HRP (1:5000, Santa Cruz) or goat anti-mouse IgG-HRP (1:3000, Santa Cruz for β-actin) were applied subsequently. Membranes from both heart tissues and cells were developed with SuperSignal West Pico Plus Chemiluminescent substrate (Thermo Scientific), acquired with ChemiDoc Touch (Bio-Rad) and analyzed using Image Lab software (Bio-Rad). β-Actin was used for loading control of cell VE-cadherin expression and total proteins were used for loading control of VE-cadherin and RXFP1 expression from heart tissues [9, 37].

Immunofluorescent staining for VE-cadherin expression

The LV from sham-operated, IR (1 h/24 h) alone and IR + relaxin treated mice was collected, embedded in OCT and frozen at − 80 °C. Fresh-frozen LVs were cut into 5 µm sections, placed on glass slides and then fixed with 4% paraformaldehyde for 20 min. After 3 times washes with PBS, tissue sections were blocked in 10% normal goat serum (ZSGB-BIO) and then incubated with primary antibody against VE-cadherin (1:500, Abcam) for 2 h at room temperature. LV sections were then incubated with Alexa Fluor 488-conjugated secondary antibody (1:300, Abcam) for 1 h. A laser scanning confocal microscope (Leica TCS SP8) was used for image acquisition. At least 6–8 images from the ischemic area under 20 × magnification per LV were acquired. VE-cadherin positive stained area was measured using Image-Pro Plus software (Media Cybernetics) and expressed as percentage of VE-cadherin positive stained area in per high magnification area of the LV.

Statistical analysis

All data were expressed as mean ± SEM unless specified otherwise. Graphpad Prism (version 6.02) was used for analysis. One-way and two-way ANOVA were used for overall significance followed by Bonferroni's multiple comparison post hoc test. $P < 0.05$ was considered statistically significant. All data acquisition and analyses were in a blind fashion.

Results

Relaxin therapy attenuated MVO but had no influence on infarct size

We initially conducted a pilot experiment to define experimental conditions by which MVO could be more readily detected. Mice ($n = 5$–6 per group) were operated to induce ischemia with various durations (1 h, 2 h and 4 h) followed by reperfusion. Based on thioflavin-S fluorescence images (Supplemental Fig. 2), 4 h ischemia induced more severe MVO determined by the presence of sizable

no-reflow zone within the AAR compared to 1 h and 2 h ischemia following by reperfusion. We, therefore, elected the 4 h/24 h IR protocol for the MVO study. Relaxin was given at 50 mg/kg. Contour analysis of LV sections demonstrated a significantly smaller low- or no-reflow area (by 38%) in relaxin versus vehicle treated groups ($P < 0.05$, Fig. 2a), indicating a reduced extent of MVO.

In another batch of mice subjected to 1 h/24 h IR, histological analysis from dually stained (Evans blue and TTC staining) LV sections revealed lack of effect by relaxin therapy on infarct size as percentage of AAR (Fig. 2c) with the size of AAR comparable between the two groups.

Relaxin therapy increased lumen-opening capillaries in the ischemic myocardium

Fluorescent histological staining was used to visualize lumen-open and lumen-close capillaries in the border zone of the infarct myocardium and one representative image demonstrated the capillary lumen changes in the non-infarct zone, the border zone and the infarct zone (Supplementary Fig. 3). Quantitative data demonstrated that IR (1 h/24 h) injury markedly reduced capillary lumen-opening rate, whilst relaxin therapy increased the count of lumen-opened capillaries by 29% ($P < 0.05$, Fig. 3).

Relaxin therapy reduced MVL in the ischemic myocardium

Next, we investigated if relaxin treatment also simultaneously mitigated IR-induced MVL. Mice subjected to IR (1 h/24 h) were treated with vehicle (saline) or relaxin (50 µg/kg). IR resulted in leakage of Evans blue into the ischemic myocardium in a massive quantity (Fig. 4a). Compared with the vehicle group, relaxin treated mice had 56% reduction of Evans blue content in the ischemic myocardium by chromatography ($P = 0.0003$, Fig. 4a). This effect was further confirmed by histological image analysis showing that the area of total MVL (i.e. dark- and light-Evans blue stained areas) was significantly smaller in relaxin than vehicle treated groups, which was largely attributable to reduced area with severe MVL (i.e. dark-Evans blue stained area, $P < 0.05$, Fig. 4b, c), implying an attenuated MVL. The area with mild leakage (i.e. light-Evans blue staining) was comparable between the two groups.

Relaxin therapy inhibited inflammatory responses

The severity of inflammation in response to IR was determined by immunohistochemical detection of the density of inflammatory cells in hearts, plasma levels of inflammatory cytokines, and by gene expression of inflammatory cytokines in hearts with IR (1 h/48 h). CD45 + leukocytes in the ischemic area were identified

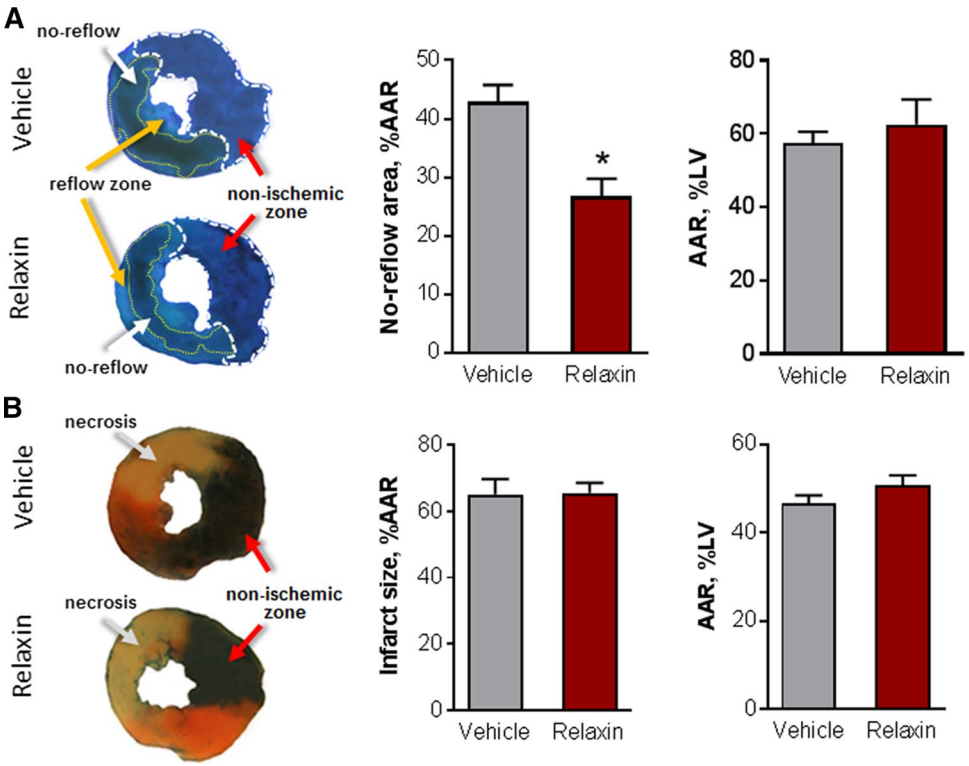

Fig. 2 Effect of relaxin treatment on no-reflow size or infarct size post ischemia–reperfusion (IR). **a** Representative cross-sectional images of the left ventricular (LV) showing no-reflow regions indicated by the absence of thioflavin-S fluorescence (white arrows and fine yellow lines) within the ischemic area that consists of both no-reflow (white arrows) and reflow zones (yellow arrows) following IR (4 h/24 h). *AAR* area-at-risk, $n = 7$–8/group. $^*P < 0.05$ vs. vehicle. **b** Representative LV cross-sectional images dual-stained with Evans blue and triphenyltetrazolium chloride for determination of AAR and infarct size. Infarct size is expressed as percentage of AAR. Mice were subjected to IR (1 h/24 h). $n = 6$–7/group

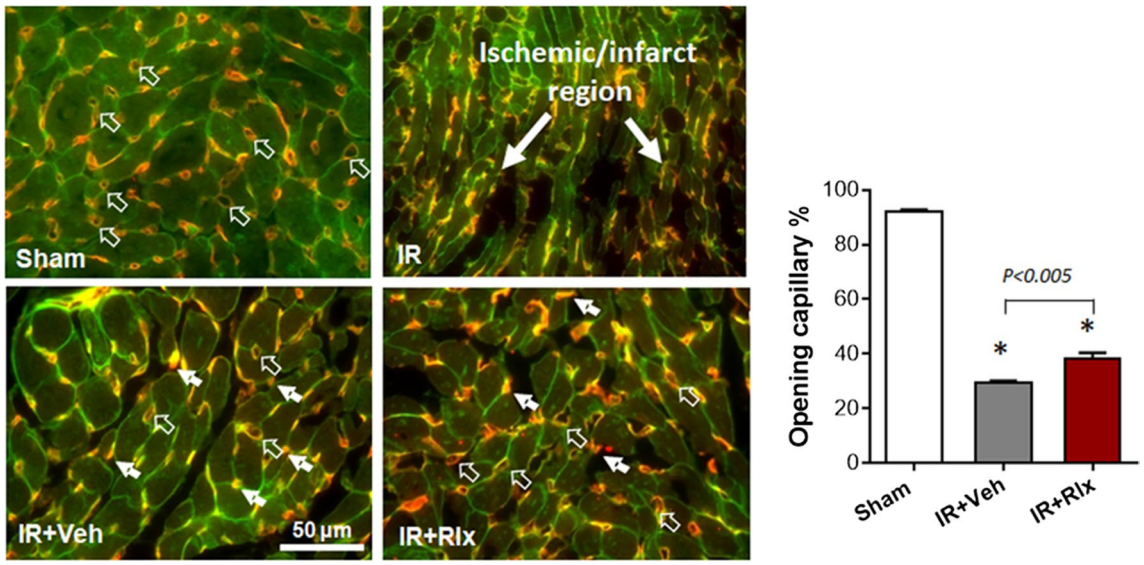

Fig. 3 Influence of relaxin therapy on lumen-open capillaries in the ischemic myocardium. Representative immunohistochemical images showing capillaries in normal myocardium or within the border zone of the infarct area. Mice were subjected to sham-operation or ischemia–reperfusion (IR, 1 h/24 h). An image (IR) depicts abnormal structures of the infarct region. Open arrows: lumen-open capillaries; solid arrows: lumen-close capillaries. Group data are expressed as percentage of lumen-opening capillaries in total counted number of capillaries (× 20 magnification). *Rlx* relaxin, *Veh* vehicle. $n = 7–8$/group, scare bar 50 µm. $^{*}P < 0.05$ vs. sham

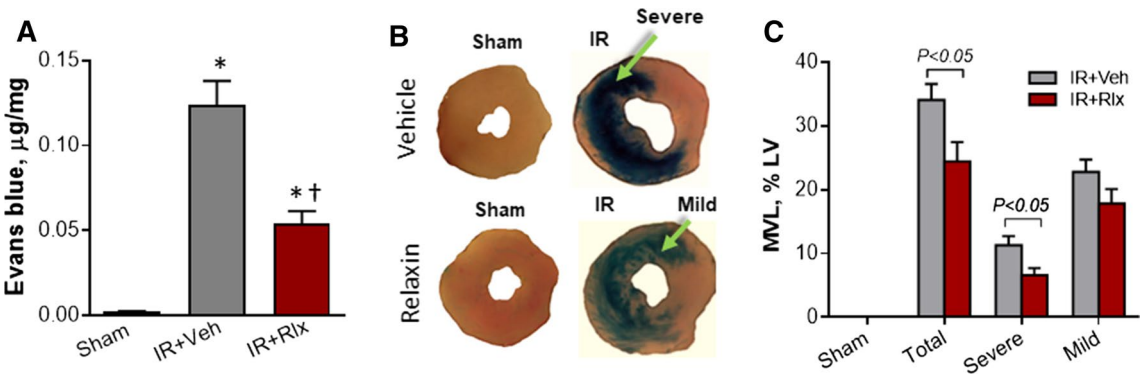

Fig. 4 Effect of relaxin therapy on ischemia–reperfusion (IR)-induced microvascular leakage (MVL). **a** IR (1 h/24 h) resulted in a massive leakage of Evans blue (EB), which was quantified chromatographically after EB extraction from the ischemic myocardium. $n = 5$ for sham, 25 for vehicle (Veh)- and 18 for relaxin (Rlx)-treated group. $^{*}P < 0.05$ vs. sham, $^{\dagger}P < 0.05$ vs. IR + Veh. **b** Representative cross-sectional images of the left ventricle (LV) from sham-operated mice and mice with IR. Relaxin treated heart exhibited a reduced extent of EB staining in the ischemic myocardium relative to vehicle-treated heart. **c** Severity of MVL was also assessed by contour analysis of regions with dark blue staining (severe leakage) or light blue staining (mild leakage), separately and expressed as percentage of total LV sectional area. $n = 6–8$/group

with immunofluorescent staining of frozen LV sections. There was a robust increase in the density of leukocytes in vehicle-treated group, and relaxin therapy reduced the density by approximately 30% ($P < 0.01$, Fig. 5a). Following IR, mRNA levels of IL-1β, IL-6, TNFα and MCP-1 by qPCR were increased by 14-, 53-, 35- and 67-folds, respectively, over the sham values. Relaxin treatment significantly downregulated expression of IL-1β, IL-6 and MCP-1 by 55–60% without effect on TNFα expression versus vehicle treated group (Fig. 5b). Further, selected inflammatory biomarkers were measured by ELISA using plasma samples collected from the same batch of mice. Levels of IL-1β and IL-6, but not TNFα were elevated after IR injury, relaxin treatment reduced the level of IL-1β and had a trend to a decreased IL-6, but had no effect on TNFα (Fig. 5c). As VEGF is a key factor determining vascular permeability [18, 47], its expression at the mRNA level was also determined. Compared to sham

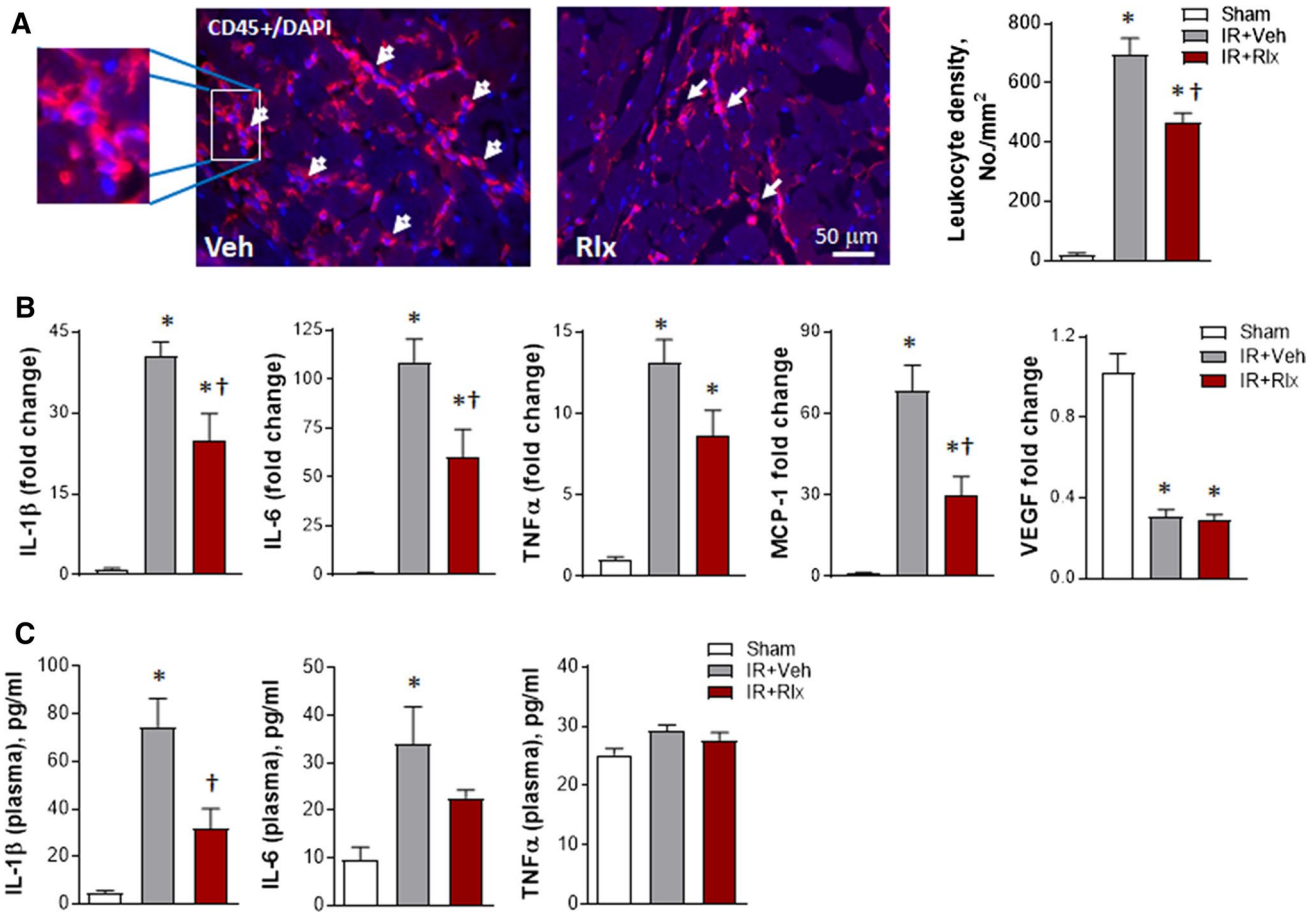

Fig. 5 Effect of relaxin therapy on inflammatory response in the heart subjected to ischemia–reperfusion (IR, 1 h/48 h). **a** Representative histological images showing CD45 + leukocytes (arrows, CD45 staining as purple colour and blue DAPI staining indicates nuclei) in the ischemic myocardium and grouped data from quantitative analysis. $n = 6$/group. *Rlx* relaxin, *Veh* vehicle. **b** Changes in gene expression of inflammatory cytokines in the ischemic myocardium by quantitative real-time PCR. Interleukins (IL-1β, IL-6), tumor necrosis factor α (TNFα), monocyte chemoattractant protein-1 (MCP1) and vascular endothelial growth factor (VEGF). $n = 8$/group. **c** Changes in plasma levels of inflammatory cytokines following I/R. $n = 8$/group. $^{*}P < 0.05$ vs. sham, $^{\dagger}P < 0.05$ vs. IR + Veh group

values, IR was associated with a 70% reduction of VEGF expression, relaxin did not reverse such change (Fig. 5b).

Relaxin therapy alleviated chronic cardiac remodelling

To study the influence of relaxin therapy on chronic cardiac remodeling, animals were subjected to IR (1 h/2 weeks), relaxin was delivered via an implanted minipump (50 μg/kg) for 2 weeks. Echocardiography was performed at the baseline and 2 weeks after IR. Mice with IR exhibited LV dilatation evidenced by increased LV areas and volumes at end-systole and end-diastole, which was associated with significant decline in EF (Table 1, all $P < 0.05$ vs. baseline). In mice treated with relaxin, LV areas and volumes at end-systole and end-diastole were slightly increased compared to baseline values but these changes were statistically insignificant. Comparison with untreated mice, relaxin treated mice had a significantly better EF and a trend for a smaller LV area or volume at the end-systole (Table 1).

To assess effect of relaxin on organ weight and cardiac fibrosis, after 2-week echocardiography, these mice were terminated at 4 weeks and the heart and lungs were harvested and weighed. In vehicle treated IR group, tibia-normalized weights of the heart and lung were increased (Table 2). Weights of the LV and right ventricle, but not atria or lungs, were reduced by relaxin treatment (Table 2, $P < 0.05$ vs. vehicle group). Histological analysis showed a comparable collagen content (scar tissue) in the myocardium of both vehicle and relaxin treated groups 4 weeks after IR (14.2 ± 1.3% vs. 12.8 ± 0.9%, P = NS, Supplementary Fig. 4).

Table 1 Echocardiographic analysis at 2 weeks after ischemia–reperfusion (IR)

Variables	Baseline ($n=13$)	IR-vehicle ($n=9$)	IR-relaxin ($n=8$)
Long-axis 2D image			
Heart rate (bpm)	427 ± 8	514 ± 8*	546 ± 15*
LVESA (mm^2)	19.0 ± 1.2	24.5 ± 1.6*	19.8 ± 1.7
LVEDA (mm^2)	27.7 ± 1.1	32.0 ± 2.0*	28.3 ± 1.6
FAC (%)	17.4 ± 1.2	14.3 ± 1.4	15.7 ± 1.1
LVESV (μl)	45.4 ± 4.1	71.0 ± 8.1*	50.4 ± 6.9
LVEDV (μl)	80.9 ± 5.8	107.5 ± 10.9*	88.5 ± 8.0
EF (%)	47.9 ± 2.5	34.1 ± 2.6*	44.6 ± 3.6†

Data are mean ± SE

LVESA and LVEDA left ventricular end-systolic or end-diastolic area, *FAC* fractional area change, *LVESV and LVEDV* LV end-systolic or end-diastolic volume, *EF* ejection fraction

*$P < 0.05$ vs. baseline, †$P < 0.05$ vs. IR-vehicle group

Table 2 Effect of relaxin on organ weights after 4-week ischemia–reperfusion (IR) injury

Groups	BW (g)	TL (mm)	LV/TL (mg/mm)	RV/TL (mg/mm)	Atria/TL (mg/mm)	Lung/TL (mg/mm)
Sham (12)	31.5 ± 0.6	18.0 ± 0.2	4.92 ± 0.25	1.28 ± 0.08	0.83 ± 0.05	8.23 ± 0.24
IR-vehicle (9)	32.7 ± 0.5	18.4 ± 0.1*	6.70 ± 0.24*	1.50 ± 0.06*	0.87 ± 0.04*	8.46 ± 0.21*
IR-relaxin (8)	30.4 ± 0.7†	18.1 ± 0.1†	5.85 ± 0.29*†	1.33 ± 0.10†	0.80 ± 0.11	8.45 ± 0.30*

Data are mean ± SE

BW body weight, *TL* tibial length, *LV* left ventricle, *RV* right ventricle

Numbers in parentheses indicate the group size. Sham group combined vehicle and relaxin treated mice due to no difference between these interventions under this condition. *$P < 0.05$ vs. sham group, †$P < 0.05$ vs. IR-vehicle group

Relaxin reduced hyper-permeability of endothelial cells under simulated IR

IR is associated with hypoxia/re-oxygenation, enhanced oxidative stress and regional accumulation of inflammatory cytokines [16]. To directly assess effect of relaxin on hyper-permeability of endothelial cells under simulated ischemic conditions, we conducted experiments using transwell device to grow H5V cells into a monolayer. Cells were subjected to 6 h hypoxia or 6 h hypoxia following by re-oxygenation of 1 h, 6 h or 24 h, respectively, in the absence or presence of relaxin (100 ng/ml). Under normoxia conditions, addition of relaxin *per se* had no effect on the permeability measured by FITC-dextran. Hypoxia for 6 h or 6 h hypoxia following re-oxygenation (for 1 h, 6 h and 24 h, respectively) increased permeability of endothelial monolayer by 40–75% over the control value, while addition of relaxin reduced the permeability by 16–31% under these conditions (all $P < 0.05$, Fig. 6a). When cells were stimulated with H_2O_2, IL-1β or MIF, the permeability of endothelial cells was increased by 20%, 13% and 16%, respectively, which was abolished by relaxin treatment (all $P < 0.05$, Fig. 6b).

Inhibition of endothelial monolayer leakage by relaxin is NO-independent but associated with better preservation of VE-cadherin and relaxin receptor, RXFP1

As endothelial cell-derived NO plays a critical role in regulating vascular function and endothelial nitric oxide synthase (eNOS) is known to be activated by relaxin [1, 17], we investigated whether protection against endothelial hyper-permeability by relaxin is NO dependent. Endothelial cells were subjected to hypoxia (6 h) or stimulated with cytokine MIF (15 h). Then a NO scavenger, hydroxocobalamin (HXC) or combination of HXC plus relaxin, was added to the system. Addition of HXC had minimal effect on the hyper-permeability induced by hypoxia or MIF (Fig. 6c, d). Addition of relaxin abolished FITC-dextran leakage under both conditions (Fig. 6c, d), suggesting that the protection exerted by relaxin is NO-independent.

Next, we examined influence of relaxin treatment on the expression of VE-cadherin, which is an endothelial specific adhesion molecule critical for vascular permeability [48]. Using the same cell culture model with hypoxia (6 h) or ischemic myocardium from in vivo IR model (1 h/24 h),

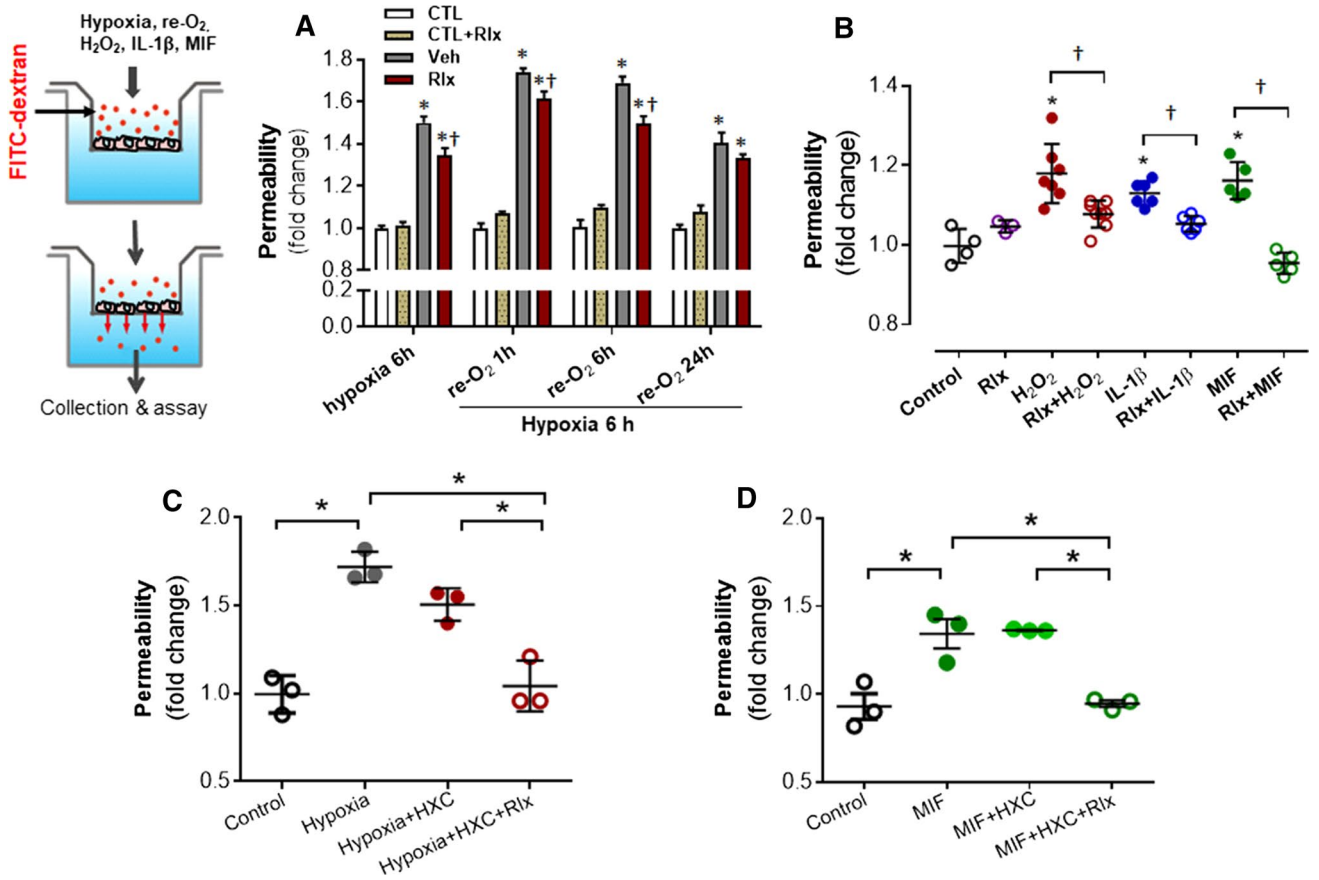

Fig. 6 Influence of relaxin on endothelial cell hyper-permeability induced by pathological stimuli. The cartoon depicts the transwell system used for the cell experiments on cultured endothelial cells forming a monolayer. **a** Endothelial monolayer was subjected to 6 h hypoxia, or hypoxia followed by re-oxygenation (re-O_2) for 1 h, 6 h and 24 h, respectively. Changes in the permeability was detected by measuring the fluorescence of indicator, FITC-dextran, in the lower chamber. $^{*}P<0.05$ vs. controls, $^{\dagger}P<0.05$ relaxin (Rlx) vs. vehicle (Veh) group. **b** Hyper-permeability of endothelial monolayer by 15 h stimulation with hydrogen peroxide (H_2O_2, 500 μm), interleukin-1β (IL-1β, 10 ng/ml) or macrophage migration inhibitory factor (MIF, 5 ng/ml), with or without addition of relaxin (Rlx, 100 ng/ml). Results are expressed as the fold changes over the control values. $^{*}P<0.05$ vs. control, $^{\dagger}P<0.05$ vs. individual stimulus. Effect of nitric oxide (NO) scavenger, hydroxocobalamin (HXC, 100 μM) on endothelial leakage was tested under conditions of hypoxia (6 h, **c**) or treatment with macrophage migration inhibitory factor (MIF 5 ng/ml, for 15 h, **d**). Relaxin was at 100 ng/ml for all data sets, $n=3$ per condition. $^{*}P<0.05$ vs. respective control

we observed a significant reduction of VE-cadherin protein expression by 20% and 67%, respectively (Fig. 7a, c). Immunofluorescent staining also detected a 43% reduction in VE-cadherin expression from hearts subjected to IR (1 h/24 h) versus sham hearts (Fig. 7b). Treatment of relaxin in cultured cells or mice with IR partially but significantly preserved VE-cadherin protein expression by both immunoblotting and immunofluorescent staining (Fig. 7a–c, all $P<0.05$). Further, we observed in the ischemic myocardium a significant reduction in the protein expression of RXFP1, which was partially prevented by relaxin therapy (66% vs. 49%, Fig. 7c, $P<0.05$). Meanwhile, RXFP1 gene expression in IR hearts was found to be dramatically downregulated, which was not affected by relaxin treatment (Fig. 7d), indicating that a higher level of RXFP1 was due to preservation of existing protein rather than by de novo protein synthesis.

Discussion

In the present study, we investigated the effect of relaxin on microvascular damage (MVO and MVL), in particular MVL both in vivo and ex vivo. A few key findings have been made. *First*, in murine IR model, relaxin therapy significantly reduced MVL, evidenced by reduced myocardial content of Evans blue as a permeability tracer and the size of the LV exhibiting severe Evans blue staining relative to controls. *Second*, the ischemic region showing no-reflow was reduced while the percentage of lumen-opening capillaries was higher in relaxin treated hearts. *Third*, the protective effect of relaxin was associated with suppressed regional inflammatory responses and modestly mitigated LV remodeling. *Finally*, in endothelial cell monolayer model, relaxin was protective against endothelial leakage evoked by

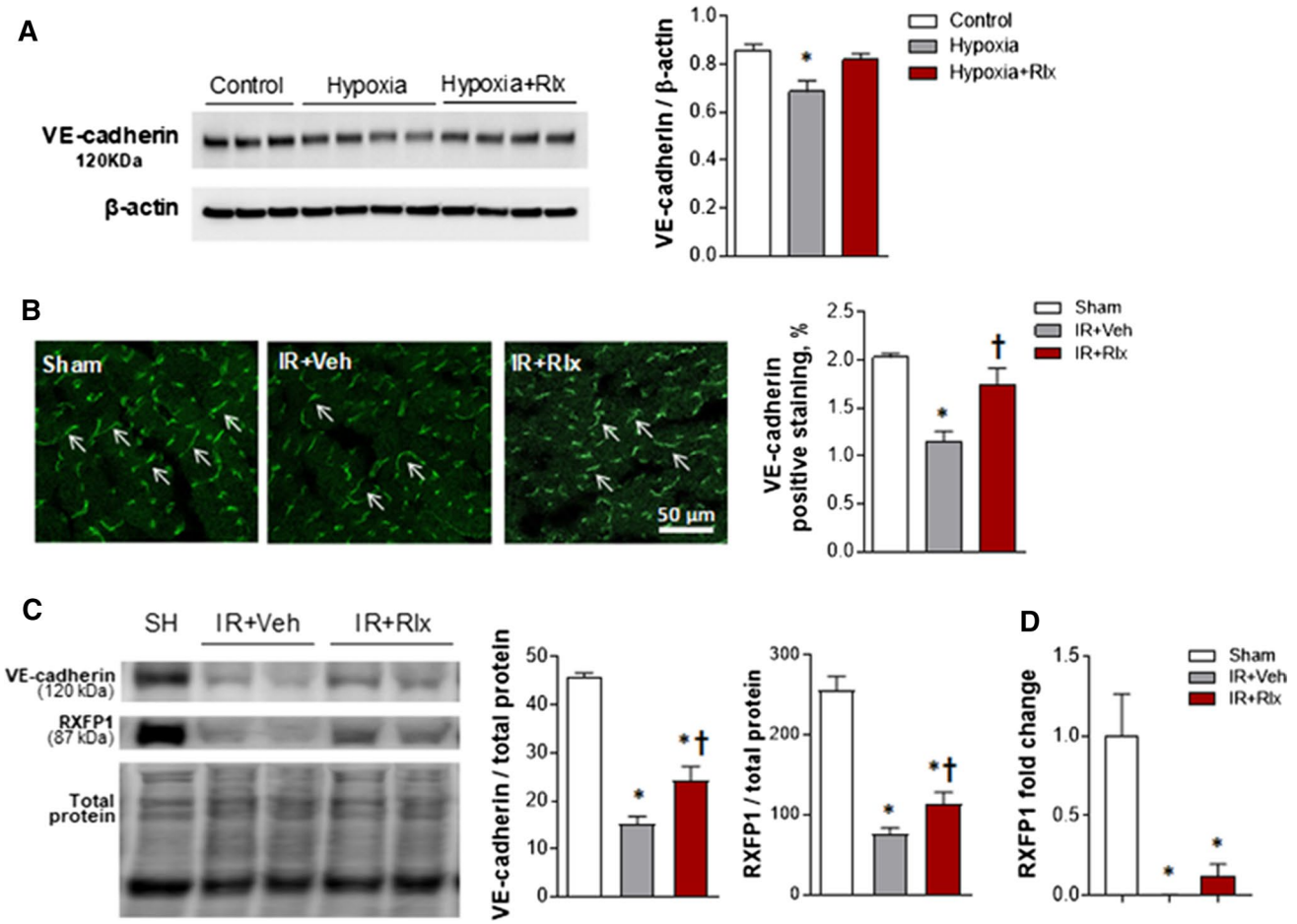

Fig. 7 Effect of relaxin therapy on expression of VE-cadherin and relaxin receptor, RXFP1, in vitro and in vivo. **a** In cultured endothelial cells, 6 h hypoxia reduced VE-cadherin abundance by 20%, which was reversed by relaxin (Rlx). $n = 3$–4/group, $^{*}P < 0.05$. vs. control. **b** VE-cadherin expression in hearts with I/R (1 h/24 h) by immunofluorescence staining of VE-cadherin (arrows) was decreased by 43%, which was partially prevented by relaxin. $n = 5$/group. $^{*}P < 0.05$ vs. sham, $^{\dagger}P < 0.05$ vs. IR + vehicle (Veh). **c** In the in vivo model of ischemia–reperfusion (IR, 1 h/24 h), VE-cadherin expression, analysed by immunoblotting and normalized by total protein signal, was reduced by 66%, and relaxin therapy partially restored VE-cadherin level. $n = 3$–5/group. $^{*}P < 0.05$. vs. sham, $^{\dagger}P < 0.05$ vs. IR + Veh. Protein expression of RXFP1 in IR hearts was reduced by 67% determined by immunoblotting, which was alleviated by relaxin therapy. $n = 3$–5/group. $^{*}P < 0.05$. vs. sham, $^{\dagger}P < 0.05$ vs. IR + Veh. **d** mRNA level of RXFP1 examined by real-time PCR in hearts of mice subjected to sham-operation or IR (1 h/24 h) with or without relaxin treatment. $n = 5$–8/group. $^{*}P < 0.05$ vs. sham

hypoxia, oxidative stress or inflammatory cytokines, effect that is independent of NO but associated with preservation of protein abundance of VE-cadherin and RXFP1.

Timely restoration of blood flow to the ischemic myocardium by different means is the primary measure to rescue jeopardized myocardium. However, IR injury occurs not only to cardiomyocytes, but also to various myocardial components including microvasculatures [13]. Being well documented by pre-clinical and clinical studies, no-reflow is a key consequence of microvascular damage commonly seen post-IR [31]. Numerous pre-clinical studies have shown cardioprotective effects of relaxin in different disease settings including IR occurring to the heart or other organs [15]. However, to the best of our knowledge, MVO and MVL have not been investigated in these studies. We examined whether relaxin offers protection against IR-induced microvascular damage using several independent techniques: contour analysis of areas of Evans blue stained myocardium (for MVL) or area absence of thioflavin-S fluorescence (for MVO), chemical assay of tissue content of Evans blue (for MVL), and percentage of lumen-opaque/closed capillaries (for MVO). Data from these measures consistently showed that relaxin therapy protects against microvascular damage with reduction in the size of MVO or the severity of MVL. Importantly, relaxin not only mitigates MVO, but also limits microvascular hyper-permeability i.e. MVL. As far as we are aware, this is the first study to show simultaneous reduction of MVO and MVL by a therapeutic intervention.

The underlying mechanism responsible for this microvascular protection was further explored. IR induced a

marked influx of leukocytes into the ischemic myocardium that is controlled by staged events of regional accumulation of chemokines, traffic signals and adhesion molecules that mediate leukocyte rolling, adhesion and extravasation [16, 49]. We observed for the first time a substantial lumen-opaque/closed capillaries in the jeopardized myocardium following IR (1 h/24 h) injury, which is likely due to aggregated leukocytes and platelets. Relaxin treatment partially but significantly reduced the proportion of lumen-opaque/closed capillaries, which may be attributable to its anti-inflammation and anti-platelet activities [2, 7, 12]. Indeed, in relaxin treated hearts with IR (1 h/48 h), regional leukocytes infiltration was suppressed by over 30%. Furthermore, expression and production of selected pro-inflammatory cytokines were also reduced by relaxin. Collectively, these findings indicate the anti-inflammatory property of relaxin, which is a likely key mechanism to mitigate MVO in IR injured heart. Indeed, no-reflow area was reduced by 30% observed in relaxin treated mice subjected to IR with severe ischemic insult (i.e. 4 h ischemia).

We observed, in the same IR model, that relaxin treatment failed in limiting the infarct size. There is inconsistency regarding changes in infarct size and MVO in response to therapeutic interventions including ischemic pre- or post-conditioning or drug interventions such as relaxin. We previously reported that when expressed as percentage of AAR, the size of MVO is much smaller than that of the infarct (35% vs. 47%) [23]. The cardiac magnetic resonance imaging study in patients with MI by Mewton et al. also revealed the same difference (18% vs. 88%) [34]. This appears to indicate that MVO is a consequence of infarct. A number of studies have indicated dissociation between the changes in infarct size and no-reflow size after interventions [11, 25, 44], the causality between MVO and cardiomyocyte death remains unresolved. Our results suggest that microvascular damage, while being independent of infarct size based on the present study, might be related to other components of the myocardium that are damaged by IR and hence form drug target. Our findings also provide an insight for the significance of IR injury to non-cardiomyocyte components in determining the extent of ultimate cardiac remodeling and dysfunction.

While the significance of MVO has been appreciated clinically, post-IR MVL has only been characterized recently [23]. In the mouse IR model, we showed that the severity of MVL is dependent on the ischemic duration and that the mass of the myocardium exhibiting MVL is significantly greater than that of no-reflow or the infarct size [23]. Despite the knowledge that vascular cells express relaxin receptors and that relaxin possesses anti-inflammatory property [2, 7, 10, 43], it remains unknown whether MVL is a target of relaxin therapy. We showed that relaxin therapy following IR effectively reduced the severity of MVL determined by histological and biochemical means. This in vivo finding is novel and potentially important by extending relaxin's myocardial protection in the setting of IR to microvasculatures. To study influence of simulated IR conditions on endothelial cell permeability, we measured permeability of endothelial monolayer under conditions of hypoxia, hypoxia-reoxygenation, oxidative stress (H_2O_2) or stimulation with selected cytokines (IL-1β, MIF). These pathological stimuli induced a significant increase in the endothelial permeability measured by FITC-dextran leakage. Microvascular hyper-permeability has been implicated by studies in other models in facilitating inflammatory cell adhesion and extravascular infiltration [49]. Under these conditions, addition of relaxin largely or partially inhibited the degree of hyper-permeability. Our ex vivo findings complement to the in vivo observation of alleviated MVL and highlight that such protection is achieved by the pleotropic actions, in particular anti-inflammatory and anti-oxidative properties of relaxin [10, 15, 43]. By facilitating inflammatory infiltration, haemorrhage, oedema and liquid retention in the interstitial space, MVL *per se* is expected to worsen MVO via heightened external compression of microvasculature.

Endothelial-derived NO plays a critical role in regulating vascular function. Altered myocardial NO balance during IR is associated with endothelial dysfunction contributing to the progression of cardiac IR injury and heart failure [19]. We tested whether endothelial protection exerted by relaxin is NO-dependent using a NO scavenger, hydroxocobalamin (HXC). Addition of HXC did not exacerbate hyper-permeability of endothelial monolayer induced by hypoxia or MIF stimulation, nor to abolish relaxin-mediated protection against hyper-permeability. Thus, relaxin exerted protection in endothelial permeability appears to be NO-independent, although further experiments are required to confirm this, given that the NO-dependent mechanism has been implicated in relaxin's protection in other disease settings [15].

VE-cadherin, an endothelial-specific junctional adhesion molecule, is vital in the maintenance and control of vascular permeability and leukocyte extravasation [48, 49]. We elected to examine in cultured endothelial cells whether hypoxia influences VE-cadherin expression. We observed significant reduction in VE-cadherin protein expression, which was reversed by relaxin treatment. This ex vivo finding was replicated in the IR model in vivo by immunoblotting and immunofluorescent staining showing a markedly reduced VE-cadherin protein expression. Once again, this was partially restored by relaxin treatment. These findings indicate that relaxin prevents endothelial leakage at least in part through preservation of VE-cadherin expression. Interestingly, a significant reduction of RXFP1 expression was observed in the ischemic myocardium, which was also partially restored by relaxin therapy, implying a role of RXFP in mediating relaxin's protective signalling. It is well known

that the activation of RXFP1 activates a variety of signaling pathways including cAMP, cGMP and MAPKs as well as by altering gene expression of TGF-β, MMPs, angiogenic growth factors and endothelin receptors [43]. The preservation of RXFP1 by relaxin is not due to de novo RXFP1 gene expression since relaxin therapy had no effect on RXFP1 mRNA level, which was profoundly reduced in IR heart.

Relaxin regimen in our experimental conditions (1 h/24 h IR) failed in limiting infarct size, a finding that differs from previous reports [3, 46]. Very few studies have investigated effect of relaxin on fibrotic healing post-MI by permanent coronary occlusion. We previously reported in mice with MI that relaxin therapy at 0.5 mg/kg for 4 weeks did not alter the scar size but reduced scar density [42]. The reason remains unclear but might be related to differences in the ischemic duration. Several studies have reported reduction in infarct size by relaxin therapy in vivo [3, 38, 39, 46]. These studies adopted an IR protocol with 30-min ischemia, shorter than that in the current study (1 h), which might suggest that relaxin's infarct size-limiting effect was attenuated with prolonged ischemic duration. The anti-fibrotic property of relaxin has been reported in numerous pre-clinical studies, mainly in models of non-ischemic heart diseases [14, 32]. We extend relaxin treatment up to 2 weeks of reperfusion. By echocardiography, a better preserved LV contractile function and limited chamber dilatation were observed in relaxin treated mice with a significantly better EF and a trend of reduced chamber size at the end-systole than untreated mice. By week-4 post-IR, relaxin treated group showed a reduced heart weight. These findings suggest potential long-term benefits of relaxin therapy via alleviating microvascular damage. This effect is achieved without change in either infarct size or fibrotic size by relaxin therapy. Similar dissociation between therapeutic benefits and lack of change in the infarct size has been reported in some [11, 25, 44], but not in other studies [34, 51, 52]. These observations may indicate the independency of these two pathological phenomena at some stage of IR injury *albeit* ultimately they will contribute to each other with the course of disease progression. As pointed out in the recent reviews [27, 28], the causality between MVO and cardiomyocyte death remains unresolved. Our current results suggest that microvascular damage, while being independent of infarct size, might be related to the overall myocardial injury and hence forms a drug target. Our findings highlight the significance of IR injury to non-cardiomyocyte components in determining the extent of ultimate cardiac remodeling and dysfunction [13]. One factor should be pointed out is the variation of the area at risk (extent of ischemic injury), which may potentially influence the therapeutic effect of relaxin on MVO, MVL and myocardial necrosis [6, 23, 33]. Consistency of the area at risk between groups with different interventions is critical for these assessments. The similarity of the area at risk between relaxin treated and untreated groups in our study minimized this potential variability (Fig. 2).

In summary, relaxin therapy attenuated myocardial microvascular damage, specifically MVO and MVL, following cardiac IR injury as well as cultured cell model. This protection is not associated with limitation of infarct size, but accompanied with suppressed regional inflammatory response. A potential mechanism responsible for this protection is partially through preservation of VE-cadherin and relaxin receptor in endothelial cells, but is NO-independent. Our findings indicate the therapeutic potential of relaxin targeting on IR-induced microvascular damage, complementing to current clinical management of acute MI.

Acknowledgements This study was funded by Grants (ID1081710, ID1005329) from the National Health and Medical Research Council (NHMRC) of Australia, the Victorian Government's Operational Infrastructure Support Program, State Key Laboratory of Pathogenesis, Prevention and Treatment of High Incidence Diseases in Central Asian, China (SKL-HIDCA-2017-Y11) and Nature Science Foundation of Xinjiang (2018D01C197). XJD was NHMRC research fellow (ID1043026). The authors acknowledge Novartis AG for supply of test sample of relaxin. We acknowledge a development grant provided by the Heini Foundations.

Compliance with ethical standards

Conflict of interest The author(s) declare that they have no conflict of interest.

References

1. Bani-Sacchi T, Bigazzi M, Bani D, Mannaioni PF, Masini E (1995) Relaxin-induced increased coronary flow through stimulation of nitric oxide production. Br J Pharmacol 116:1589–1594. https://doi.org/10.1111/j.1476-5381.1995.tb16377.x
2. Bani D, Bigazzi M, Masini E, Bani G, Sacchi TB (1995) Relaxin depresses platelet aggregation: in vitro studies on isolated human and rabbit platelets. Lab Investig 73:709–716
3. Bani D, Masini E, Bello MG, Bigazzi M, Sacchi TB (1998) Relaxin protects against myocardial injury caused by ischemia and reperfusion in rat heart. Am J Pathol 152:1367–1376
4. Beiert T, Knappe V, Tiyerili V, Stockigt F, Effelsberg V, Linhart M, Steinmetz M, Klein S, Schierwagen R, Trebicka J, Roell W, Nickenig G, Schrickel JW, Andrie RP (2018) Chronic lower-dose relaxin administration protects from arrhythmia in experimental myocardial infarction due to anti-inflammatory and anti-fibrotic properties. Int J Cardiol 250:21–28. https://doi.org/10.1016/j.ijcard.2017.09.017
5. Bekkers SC, Yazdani SK, Virmani R, Waltenberger J (2010) Microvascular obstruction: underlying pathophysiology and clinical diagnosis. J Am Coll Cardiol 55:1649–1660. https://doi.org/10.1016/j.jacc.2009.12.037
6. Botker HE, Hausenloy D, Andreadou I, Antonucci S, Boengler K, Davidson SM, Deshwal S, Devaux Y, Di Lisa F, Di Sante M, Efentakis P, Femmino S, Garcia-Dorado D, Giricz Z, Ibanez B, Iliodromitis E, Kaludercic N, Kleinbongard P, Neuhauser M, Ovize M, Pagliaro P, Rahbek-Schmidt M, Ruiz-Meana M, Schluter KD, Schulz R, Skyschally A, Wilder C, Yellon DM, Ferdinandy P, Heusch G (2018) Practical guidelines for rigor and reproducibility

in preclinical and clinical studies on cardioprotection. Basic Res Cardiol 113:39. https://doi.org/10.1007/s00395-018-0696-8
7. Brecht A, Bartsch C, Baumann G, Stangl K, Dschietzig T (2011) Relaxin inhibits early steps in vascular inflammation. Regul Pept 166:76–82. https://doi.org/10.1016/j.regpep.2010.09.001
8. Carrick D, Haig C, Ahmed N, Rauhalammi S, Clerfond G, Carberry J, Mordi I, McEntegart M, Petrie MC, Eteiba H, Hood S, Watkins S, Lindsay MM, Mahrous A, Welsh P, Sattar N, Ford I, Oldroyd KG, Radjenovic A, Berry C (2016) Temporal evolution of myocardial hemorrhage and edema in patients after acute ST-segment elevation myocardial infarction: pathophysiological insights and clinical implications. J Am Heart Assoc 5:e002834. https://doi.org/10.1161/JAHA.115.002834
9. Collins MA, An J, Peller D, Bowser R (2015) Total protein is an effective loading control for cerebrospinal fluid western blots. J Neurosci Methods 251:72–82. https://doi.org/10.1016/j.jneumeth.2015.05.011
10. Conrad KP, Novak J (2004) Emerging role of relaxin in renal and cardiovascular function. Am J Physiol Regul Integr Comp Physiol 287:R250–R261. https://doi.org/10.1152/ajpregu.00672.2003
11. Dai W, Hale S, Kloner RA (2017) Delayed therapeutic hypothermia protects against the myocardial no-reflow phenomenon independently of myocardial infarct size in a rat ischemia/reperfusion model. Int J Cardiol 236:400–404. https://doi.org/10.1016/j.ijcard.2017.01.079
12. Dschietzig T, Brecht A, Bartsch C, Baumann G, Stangl K, Alexiou K (2012) Relaxin improves TNF-alpha-induced endothelial dysfunction: the role of glucocorticoid receptor and phosphatidylinositol 3-kinase signalling. Cardiovasc Res 95:97–107. https://doi.org/10.1093/cvr/cvs149
13. Du XJ (2018) Post-infarct cardiac injury, protection and repair: roles of non-cardiomyocyte multicellular and acellular components. Sci China Life Sci 31:266–276. https://doi.org/10.1007/s11427-017-9223-x
14. Du XJ, Bathgate RA, Samuel CS, Dart AM, Summers RJ (2010) Cardiovascular effects of relaxin: from basic science to clinical therapy. Nat Rev Cardiol 7:48–58. https://doi.org/10.1038/nrcardio.2009.198
15. Du XJ, Hewitson TD, Nguyen MN, Samuel CS (2014) Therapeutic effects of serelaxin in acute heart failure. Circ J 78:542–552. https://doi.org/10.1253/circj.CJ-14-0014
16. Eltzschig HK, Eckle T (2011) Ischemia and reperfusion—from mechanism to translation. Nat Med 17:1391–1401. https://doi.org/10.1038/nm.2507
17. Failli P, Nistri S, Quattrone S, Mazzetti L, Bigazzi M, Sacchi TB, Bani D (2002) Relaxin up-regulates inducible nitric oxide synthase expression and nitric oxide generation in rat coronary endothelial cells. FASEB J 16:252–254. https://doi.org/10.1096/fj.01-0569fje
18. Feng D, Nagy JA, Hipp J, Dvorak HF, Dvorak AM (1996) Vesiculo-vacuolar organelles and the regulation of venule permeability to macromolecules by vascular permeability factor, histamine, and serotonin. J Exp Med 183:1981–1986
19. Folino A, Losano G, Rastaldo R (2013) Balance of nitric oxide and reactive oxygen species in myocardial reperfusion injury and protection. J Cardiovasc Pharmacol 62:567–575. https://doi.org/10.1097/FJC.0b013e3182a50c45
20. Funaro S, Galiuto L, Boccalini F, Cimino S, Canali E, Evangelio F, DeLuca L, Paraggio L, Mattatelli A, Gnessi L, Agati L (2011) Determinants of microvascular damage recovery after acute myocardial infarction: results from the acute myocardial infarction contrast imaging (AMICI) multi-centre study. Eur J Echocardiogr 12:306–312. https://doi.org/10.1093/ejechocard/jer009
21. Gao XM, Liu Y, White D, Su Y, Drew BG, Bruce CR, Kiriazis H, Xu Q, Jennings N, Bobik A, Febbraio MA, Kingwell BA, Bucala R, Fingerle-Rowson G, Dart AM, Morand EF, Du XJ (2011) Deletion of macrophage migration inhibitory factor protects the heart from severe ischemia–reperfusion injury: a predominant role of anti-inflammation. J Mol Cell Cardiol 50:991–999. https://doi.org/10.1016/j.yjmcc.2010.12.022
22. Gao XM, Moore XL, Liu Y, Wang XY, Han LP, Su Y, Tsai A, Xu Q, Zhang M, Lambert GW, Kiriazis H, Gao W, Dart AM, Du XJ (2016) Splenic release of platelets contributes to increased circulating platelet size and inflammation after myocardial infarction. Clin Sci (Lond) 130:1089–1104. https://doi.org/10.1042/CS20160234
23. Gao XM, Wu QZ, Kiriazis H, Su Y, Han LP, Pearson JT, Taylor AJ, Du XJ (2017) Microvascular leakage in acute myocardial infarction: characterization by histology, biochemistry, and magnetic resonance imaging. Am J Physiol Heart Circ Physiol 312:H1068–H1075. https://doi.org/10.1152/ajpheart.00073.2017
24. Garlanda C, Parravicini C, Sironi M, De Rossi M, de Wainstok Calmanovici R, Carozzi F, Bussolino F, Colotta F, Mantovani A, Vecchi A (1994) Progressive growth in immunodeficient mice and host cell recruitment by mouse endothelial cells transformed by polyoma middle-sized T antigen: implications for the pathogenesis of opportunistic vascular tumors. Proc Natl Acad Sci USA 91:7291–7295. https://doi.org/10.1073/pnas.91.15.7291
25. Hale SL, Mehra A, Leeka J, Kloner RA (2008) Postconditioning fails to improve no reflow or alter infarct size in an open-chest rabbit model of myocardial ischemia–reperfusion. Am J Physiol Heart Circ Physiol 294:H421–H425. https://doi.org/10.1152/ajpheart.00962.2007
26. Hamirani YS, Wong A, Kramer CM, Salerno M (2014) Effect of microvascular obstruction and intramyocardial hemorrhage by CMR on LV remodeling and outcomes after myocardial infarction: a systematic review and meta-analysis. JACC Cardiovasc Imaging 7:940–952. https://doi.org/10.1016/j.jcmg.2014.06.012
27. Hausenloy DJ, Chilian W, Crea F, Davidson SM, Ferdinandy P, Garcia-Dorado D, van Royen N, Schulz R, Heusch G (2019) The coronary circulation in acute myocardial ischaemia/reperfusion injury: a target for cardioprotection. Cardiovasc Res 115:1143–1155. https://doi.org/10.1093/cvr/cvy286
28. Heusch G (2016) The coronary circulation as a target of cardioprotection. Circ Res 118:1643–1658. https://doi.org/10.1161/CIRCRESAHA.116.308640
29. Hirase T, Node K (2012) Endothelial dysfunction as a cellular mechanism for vascular failure. Am J Physiol Heart Circ Physiol 302:H499–H505. https://doi.org/10.1152/ajpheart.00325.2011
30. Hisaw FL, Zarrow MX (1950) The physiology of relaxin. Vitam Horm 8:151–178. https://doi.org/10.1016/S0083-6729(08)60670-6
31. Kloner RA (2011) No-reflow phenomenon: maintaining vascular integrity. J Cardiovasc Pharmacol Ther 16:244–250. https://doi.org/10.1177/1074248411405990
32. Lam M, Royce SG, Samuel CS, Bourke JE (2018) Serelaxin as a novel therapeutic opposing fibrosis and contraction in lung diseases. Pharmacol Ther 187:61–70. https://doi.org/10.1016/j.pharmthera.2018.02.004
33. Lindsey ML, Bolli R, Canty JM Jr, Du XJ, Frangogiannis NG, Frantz S, Gourdie RG, Holmes JW, Jones SP, Kloner RA, Lefer DJ, Liao R, Murphy E, Ping P, Przyklenk K, Recchia FA, Schwartz Longacre L, Ripplinger CM, Van Eyk JE, Heusch G (2018) Guidelines for experimental models of myocardial ischemia and infarction. Am J Physiol Heart Circ Physiol 314:H812–H838. https://doi.org/10.1152/ajpheart.00335.2017
34. Mewton N, Thibault H, Roubille F, Lairez O, Rioufol G, Sportouch C, Sanchez I, Bergerot C, Cung TT, Finet G, Angoulvant D, Revel D, Bonnefoy-Cudraz E, Elbaz M, Piot C, Sahraoui I, Croisille P, Ovize M (2013) Postconditioning attenuates no-reflow in STEMI patients. Basic Res Cardiol 108:383. https://doi.org/10.1007/s00395-013-0383-8

35. Moore XL, Su Y, Fan Y, Zhang YY, Woodcock EA, Dart AM, Du XJ (2014) Diverse regulation of cardiac expression of relaxin receptor by alpha1- and beta1-adrenoceptors. Cardiovasc Drugs Ther 28:221–228. https://doi.org/10.1007/s10557-014-6525-x
36. Ndrepepa G, Tiroch K, Fusaro M, Keta D, Seyfarth M, Byrne RA, Pache J, Alger P, Mehilli J, Schomig A, Kastrati A (2010) 5-Year prognostic value of no-reflow phenomenon after percutaneous coronary intervention in patients with acute myocardial infarction. J Am Coll Cardiol 55:2383–2389. https://doi.org/10.1016/j.jacc.2009.12.054
37. Nie X, Li C, Hu S, Xue F, Kang YJ, Zhang W (2017) An appropriate loading control for western blot analysis in animal models of myocardial ischemic infarction. Biochem Biophys Rep 12:108–113. https://doi.org/10.1016/j.bbrep.2017.09.001
38. Nistri S, Cinci L, Perna AM, Masini E, Mastroianni R, Bani D (2008) Relaxin induces mast cell inhibition and reduces ventricular arrhythmias in a swine model of acute myocardial infarction. Pharmacol Res 57:43–48. https://doi.org/10.1016/j.phrs.2007.11.001
39. Perna AM, Masini E, Nistri S, Briganti V, Chiappini L, Stefano P, Bigazzi M, Pieroni C, Bani Sacchi T, Bani D (2005) Novel drug development opportunity for relaxin in acute myocardial infarction: evidences from a swine model. FASEB J 19:1525–1527. https://doi.org/10.1096/fj.04-3664fje
40. Qin CX, May LT, Li R, Cao N, Rosli S, Deo M, Alexander AE, Horlock D, Bourke JE, Yang YH, Stewart AG, Kaye DM, Du XJ, Sexton PM, Christopoulos A, Gao XM, Ritchie RH (2017) Small-molecule-biased formyl peptide receptor agonist compound 17b protects against myocardial ischaemia–reperfusion injury in mice. Nat Commun 8:14232. https://doi.org/10.1038/ncomms14232
41. Reffelmann T, Kloner RA (2002) Microvascular reperfusion injury: rapid expansion of anatomic no reflow during reperfusion in the rabbit. Am J Physiol Heart Circ Physiol 283:H1099–H1107. https://doi.org/10.1152/ajpheart.00270.2002
42. Samuel CS, Cendrawan S, Gao XM, Ming Z, Zhao C, Kiriazis H, Xu Q, Tregear GW, Bathgate RA, Du XJ (2011) Relaxin remodels fibrotic healing following myocardial infarction. Lab Investig 91:675–690. https://doi.org/10.1038/labinvest.2010.198
43. Sarwar M, Du XJ, Dschietzig TB, Summers RJ (2017) The actions of relaxin on the human cardiovascular system. Br J Pharmacol 174:933–949. https://doi.org/10.1111/bph.13523
44. Skyschally A, Amanakis G, Neuhauser M, Kleinbongard P, Heusch G (2017) Impact of electrical defibrillation on infarct size and no-reflow in pigs subjected to myocardial ischemia–reperfusion without and with ischemic conditioning. Am J Physiol Heart Circ Physiol 313:H871–H878. https://doi.org/10.1152/ajpheart.00293.2017
45. Stark K, Pekayvaz K, Massberg S (2018) Role of pericytes in vascular immunosurveillance. Front Biosci (Landmark Ed) 23:767–781. https://doi.org/10.2741/4615
46. Valle Raleigh J, Mauro AG, Devarakonda T, Marchetti C, He J, Kim E, Filippone S, Das A, Toldo S, Abbate A, Salloum FN (2017) Reperfusion therapy with recombinant human relaxin-2 (serelaxin) attenuates myocardial infarct size and NLRP3 inflammasome following ischemia/reperfusion injury via eNOS-dependent mechanism. Cardiovasc Res 113:609–619. https://doi.org/10.1093/cvr/cvw246
47. van Nieuw Amerongen GP, van Hinsbergh VW (2002) Targets for pharmacological intervention of endothelial hyperpermeability and barrier function. Vasc Pharmacol 39:257–272. https://doi.org/10.1016/S1537-1891(03)00014-4
48. Vestweber D (2008) VE-cadherin: the major endothelial adhesion molecule controlling cellular junctions and blood vessel formation. Arterioscler Thromb Vasc Biol 28:223–232. https://doi.org/10.1161/ATVBAHA.107.158014
49. Weber C, Fraemohs L, Dejana E (2007) The role of junctional adhesion molecules in vascular inflammation. Nat Rev Immunol 7:467–477. https://doi.org/10.1038/nri2096
50. White DA, Su Y, Kanellakis P, Kiriazis H, Morand EF, Bucala R, Dart AM, Gao XM, Du XJ (2014) Differential roles of cardiac and leukocyte derived macrophage migration inhibitory factor in inflammatory responses and cardiac remodelling post myocardial infarction. J Mol Cell Cardiol 69:32–42. https://doi.org/10.1016/j.yjmcc.2014.01.015
51. Yetgin T, Uitterdijk A, Te Lintel Hekkert M, Merkus D, Krabbendam-Peters I, van Beusekom HMM, Falotico R, Serruys PW, Manintveld OC, van Geuns RM, Zijlstra F, Duncker DJ (2015) Limitation of infarct size and no-reflow by intracoronary adenosine depends critically on dose and duration. JACC Cardiovasc Interv 8:1990–1999. https://doi.org/10.1016/j.jcin.2015.08.033
52. Zhao XJ, Liu XL, He GX, Xu HP (2014) Effects of single-dose atorvastatin on interleukin-6, interferon gamma, and myocardial no-reflow in a rabbit model of acute myocardial infarction and reperfusion. Braz J Med Biol Res 47:245–251. https://doi.org/10.1590/1414-431X20132999